

INTRODUCTION

This study presents the experimental results of an investigation on the effects of nanosilica (NS) on the material characteristics of printable mortars used for additive manufacturing. Printable cement mortars based on Ordinary Portland Cement, limestone filler and silica sand were modified with different dosages of nanosilica (from 2 % to 6 % by weight of binder) and its influence on their hydration, rheological, mechanical and transport properties was assessed. Accordingly, the hydration, rheological, mechanical and transport properties of printable mortars were analyzed. In addition, to assess the pore characteristics of the 3D printed mortar, a comprehensive microstructural analysis utilizing micro-computed tomography (micro-CT), and scanning electron microscopy (SEM) was also performed.

MIXTURE DESIGN

Table 1. Ratio of components in printable mortar mixtures

Mix	Cement	Fine limestone powder	Coarse limestone powder	Silica sand	Water	SP* [%]	Thickening agent* [%]	NS* [%]
0NS	1	0.3	0.5	1.8	0.52	0.24	0.09	-
2NS	1	0.3	0.5	1.8	0.52	0.24	0.09	2
3NS	1	0.3	0.5	1.8	0.52	0.24	0.09	3
4NS	1	0.3	0.5	1.8	0.52	0.27	0.09	4
6NS	1	0.3	0.5	1.8	0.52	0.28	0.09	6

TESTING METHODS

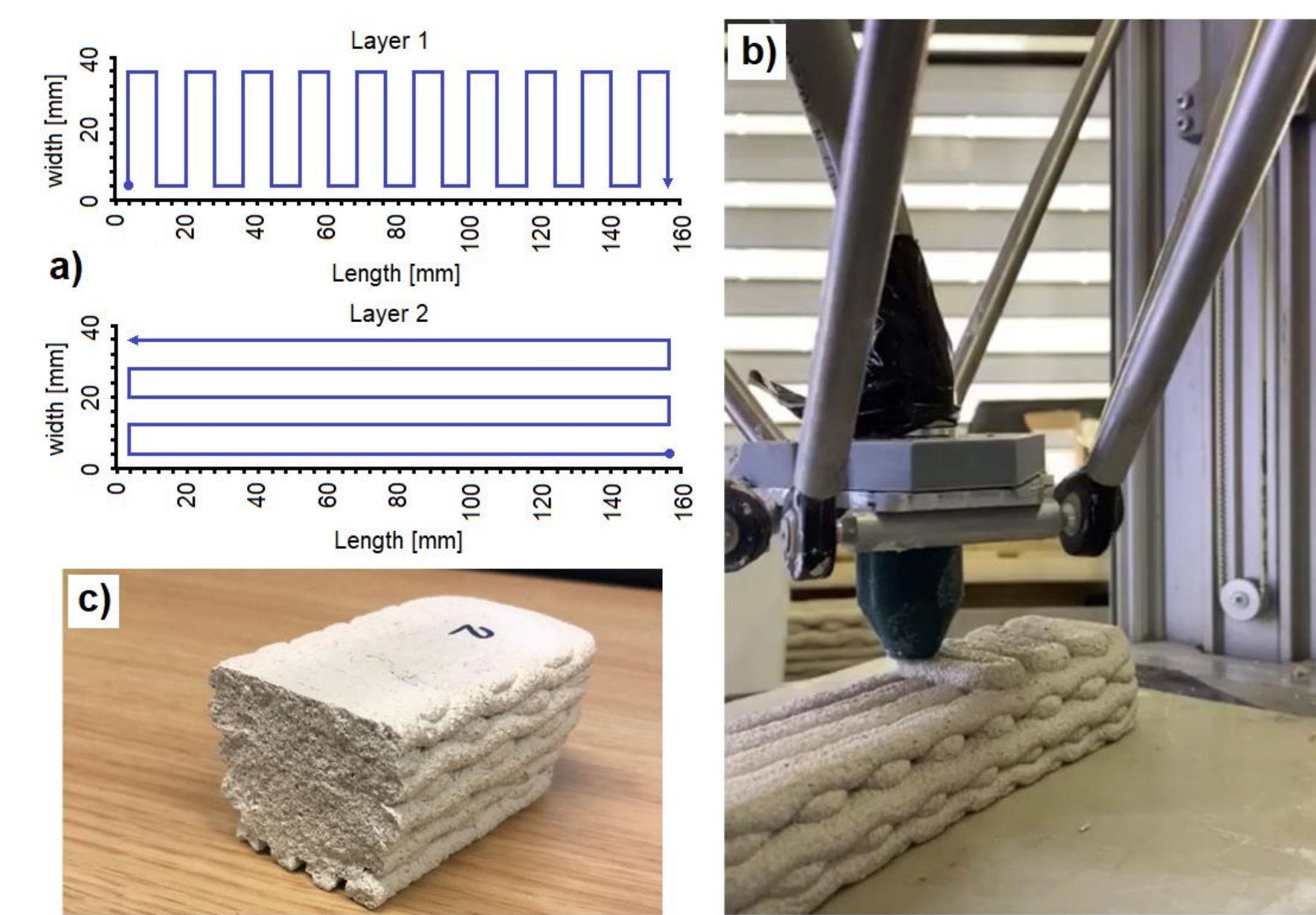


Figure 1. Printing path of first two layers of a prism (a), specimen during printing (b), printed element used for compressive strength evaluations (c).

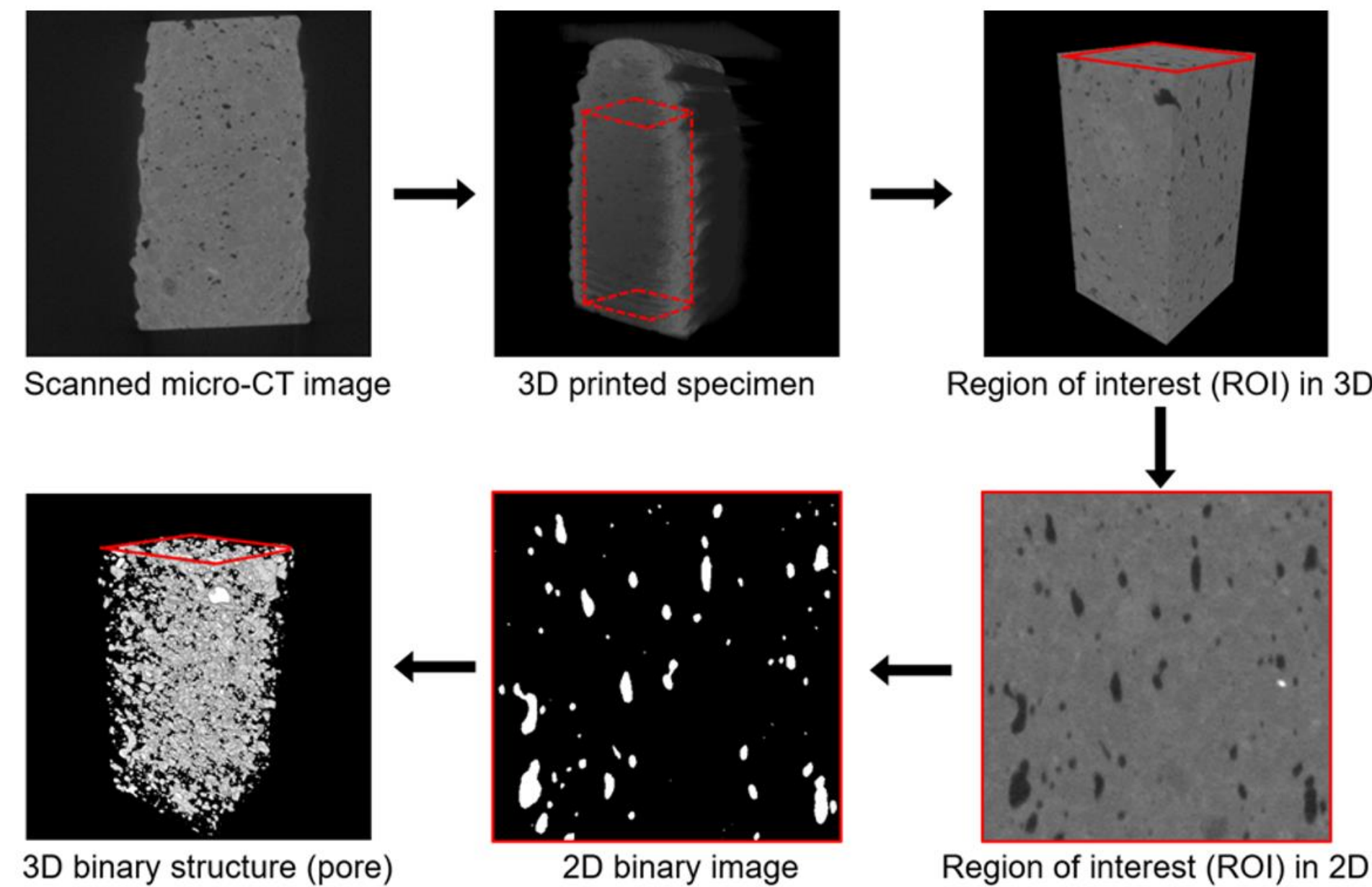


Figure 2. Micro-CT imaging procedure for classifying pore structure (3NS) (Note: in the 2D and 3D binary images, the white represents pores within the specimen.)

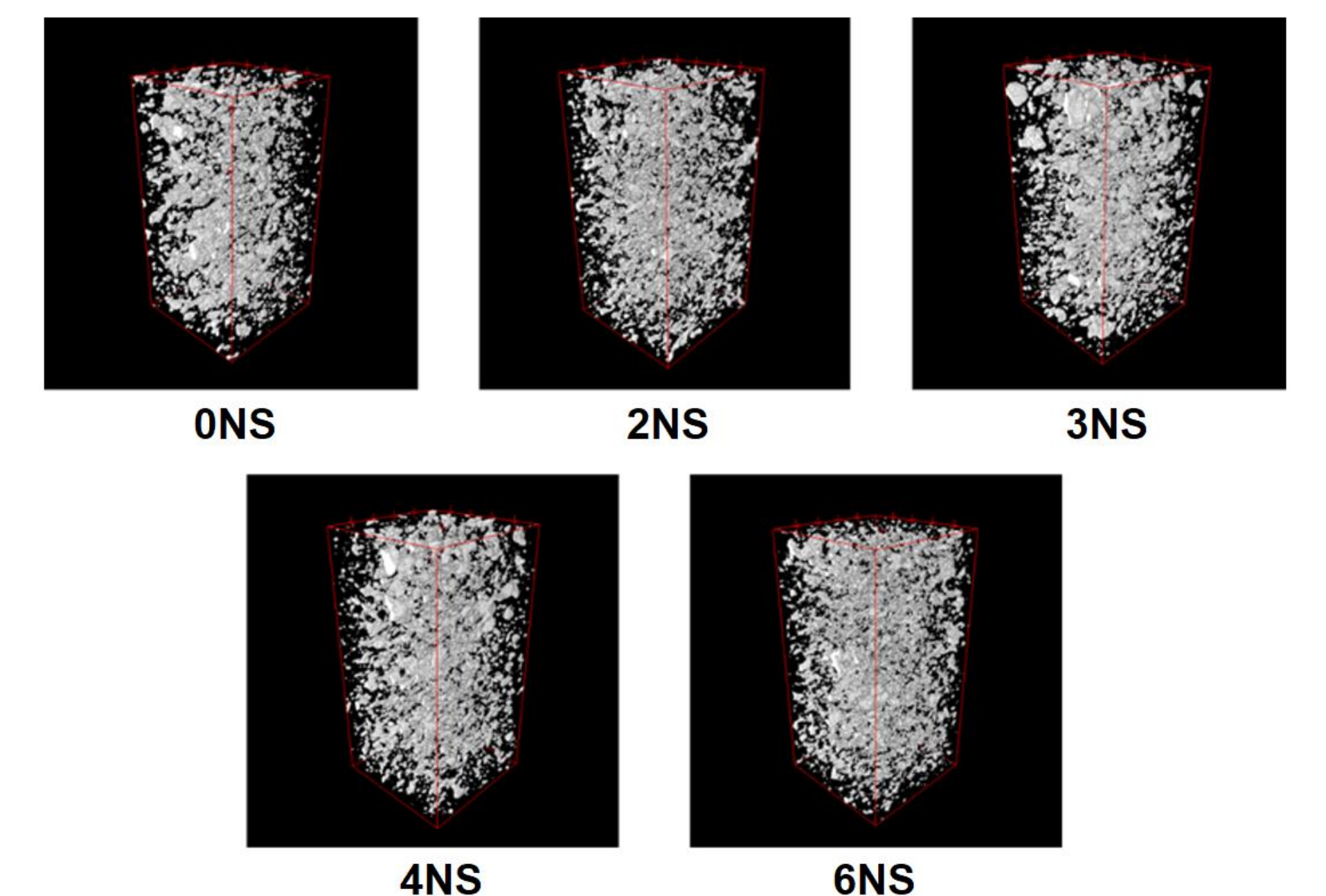


Figure 3. Void size distribution in 3D printed specimens obtained from micro-CT.

RESULTS

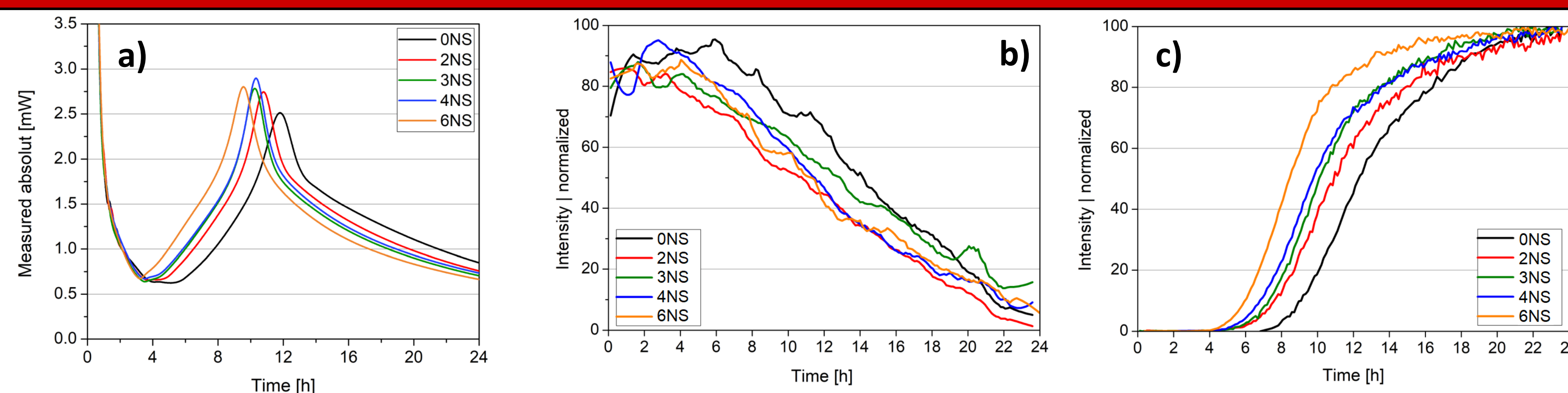


Figure 4. Heat flow (a) and normalized reflex intensity development measured by in-situ XRD of 024 C3S reflex (b) and 001 portlandite reflex (c).

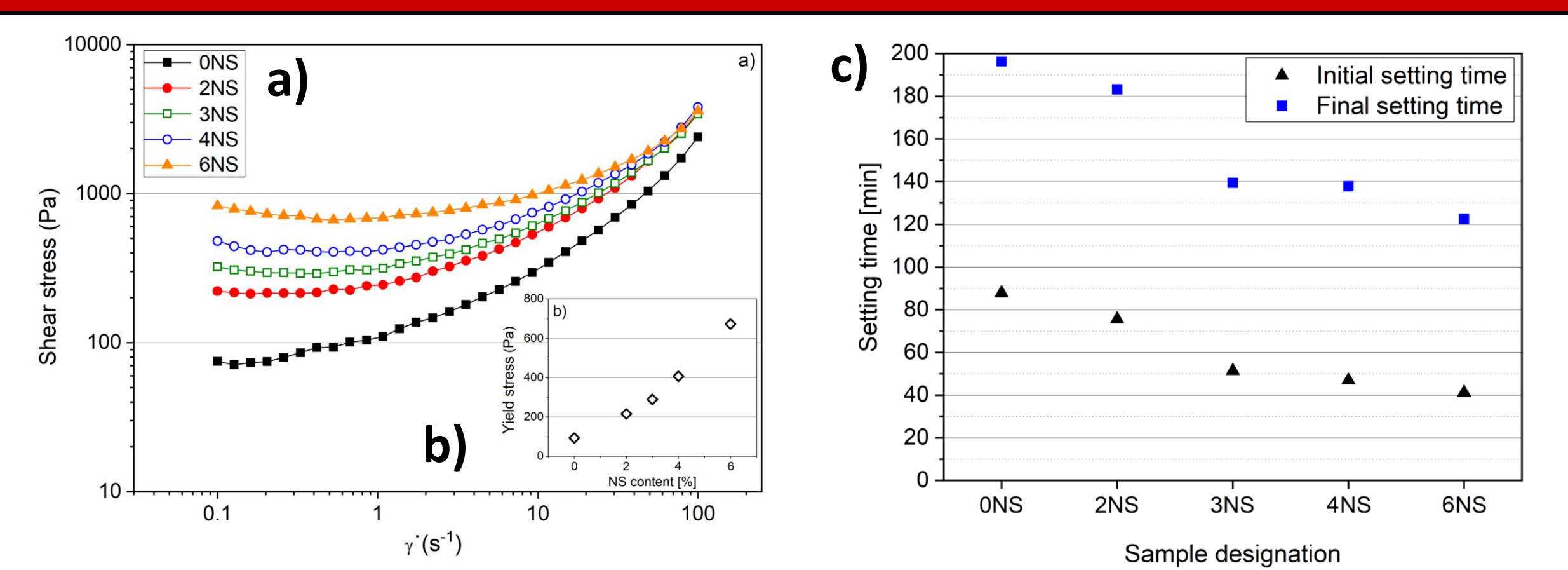


Figure 5. Shear-stress as a function of the shear-rate of printable mortars with different NS contents (a) and yield-stress at 0.4 s⁻¹ vs. NS dosage (b), setting times obtained with an ultrasonic device (c).

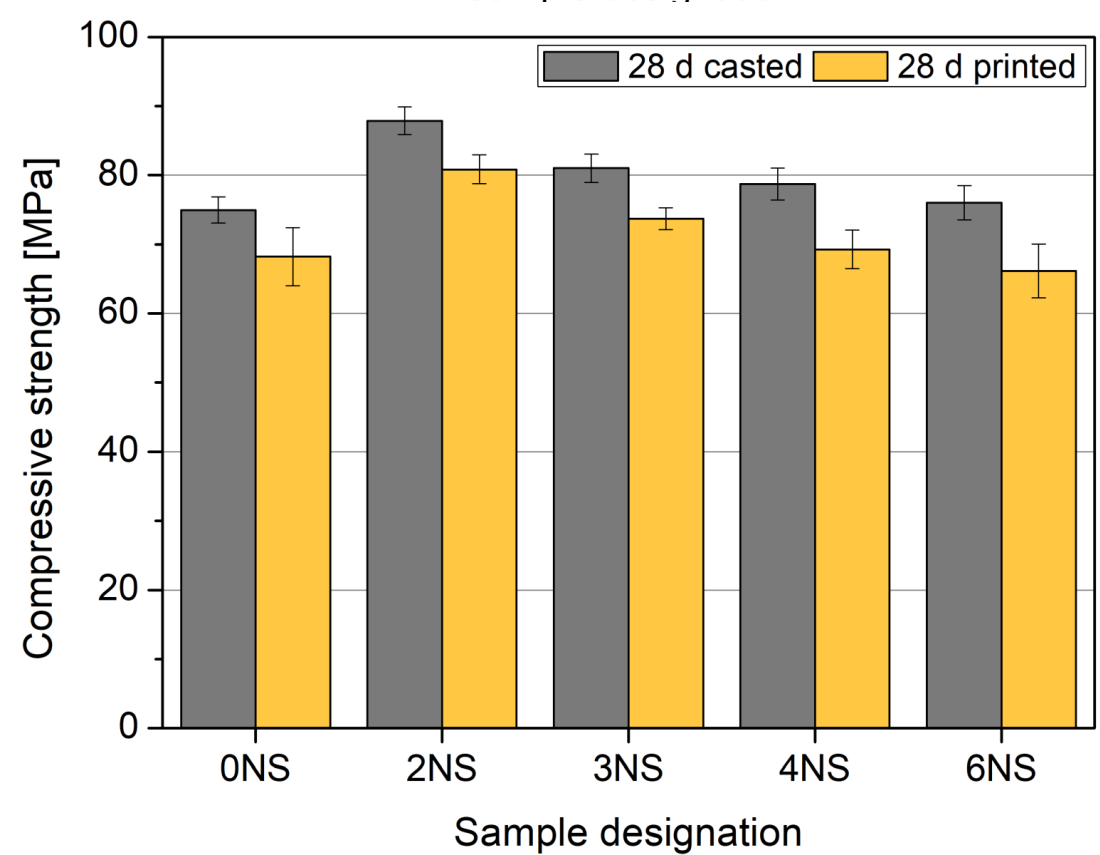
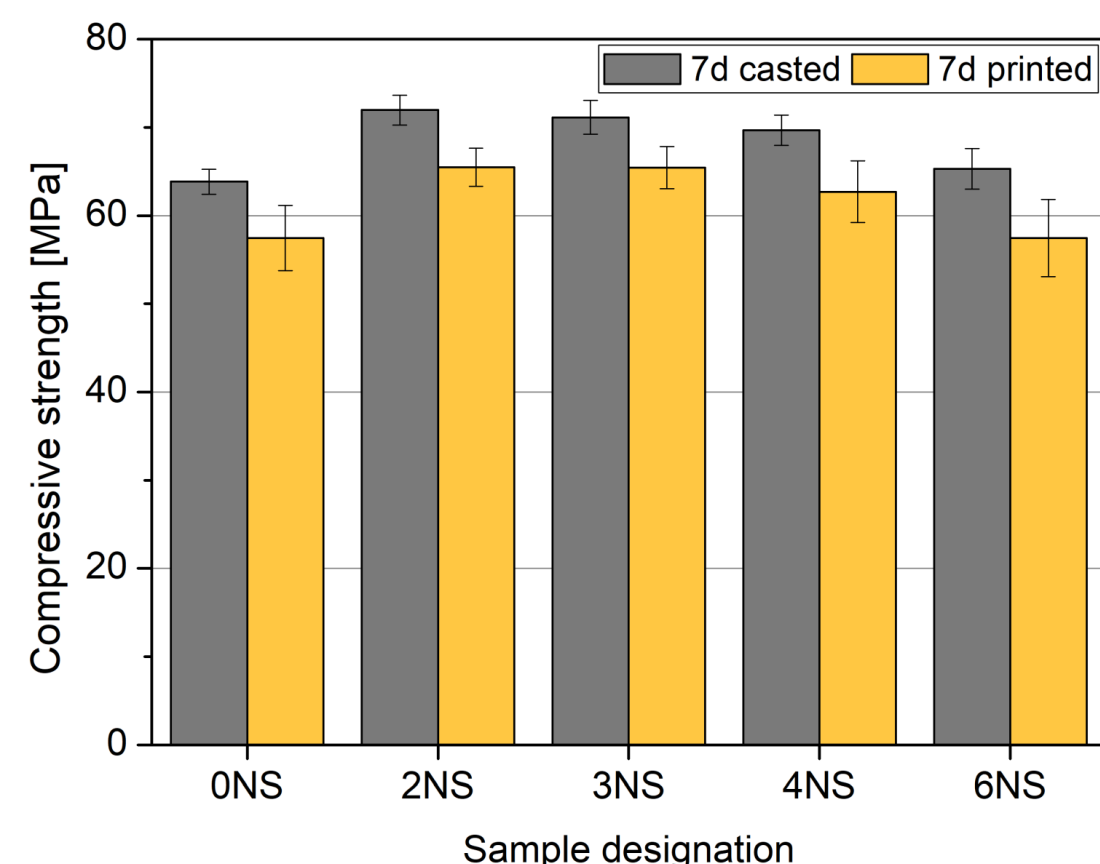


Figure 6. Water accessible porosity and water absorption coefficient of printable mortars.

Figure 8. Compressive strength after 7 d and 28 d.

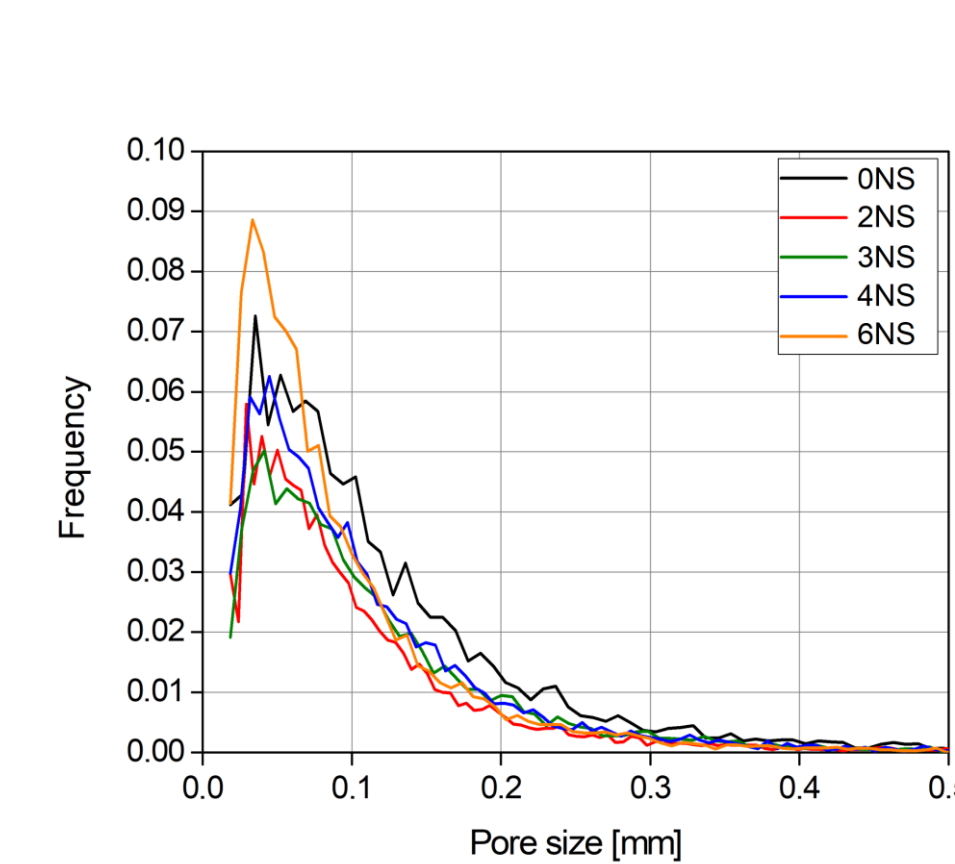
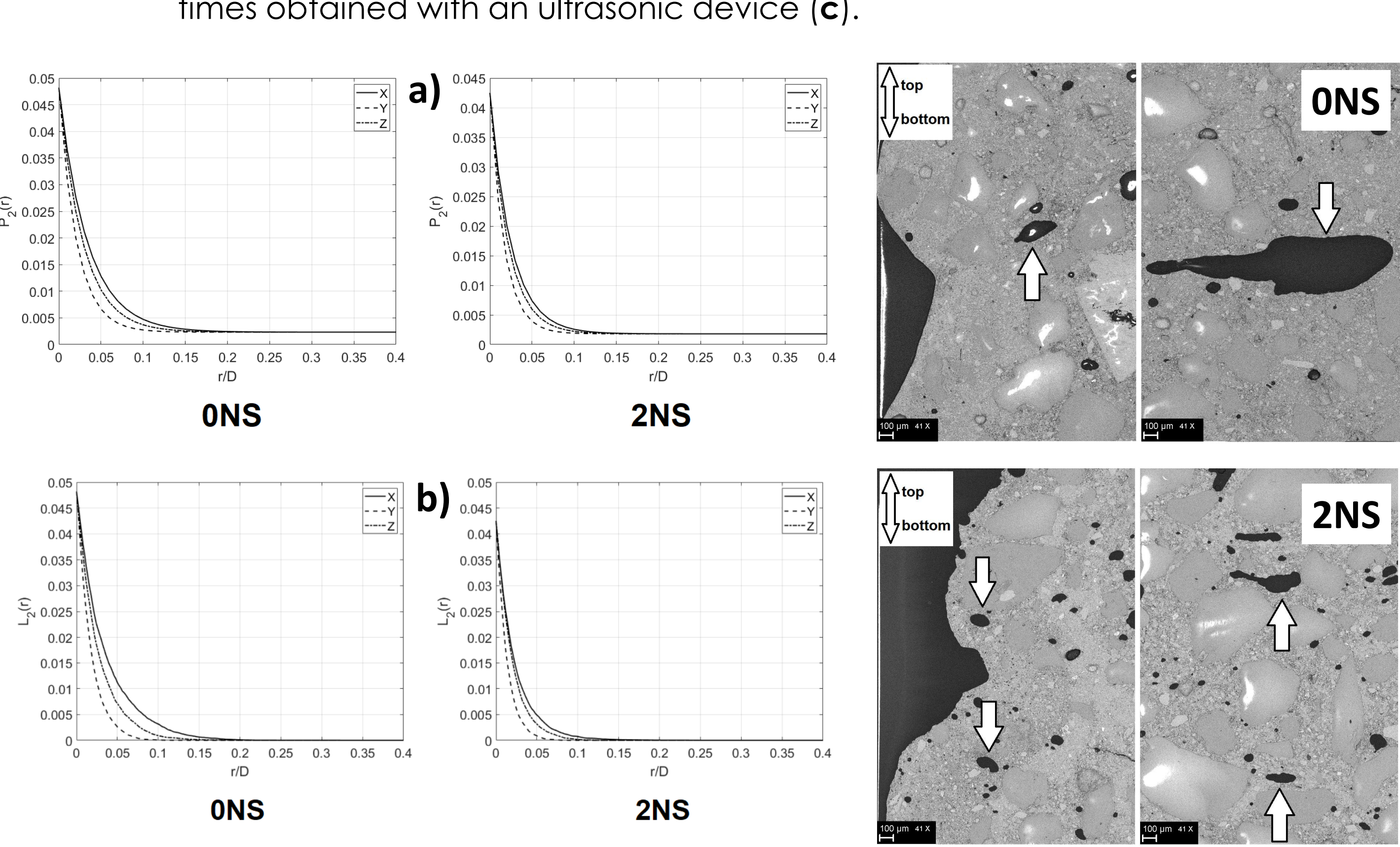


Figure 7. Void size distribution in 3D printed specimens obtained from micro-CT.

Figure 9. Two-point correlation function (a) and lineal-path function (b) of 0NS and 2NS in x, y and z directions (Note: D is the specimen length, while r is the distance between two random points.)



CONCLUSIONS

The study showed that NS accelerates significantly the setting and hardening of printable mortar, while reducing its open time. Moreover, an increment of yield stress, together with an increment in NS dosage, was found to have occurred. The incorporation of an optimal NS dosage results in a noticeable increase in the compressive strength and alteration of the pore structure. Moreover, transport properties of the produced mortar are significantly improved due to incorporation of NS. In addition to the microstructure refinement, Micro-CT and scanning electron microscopy (SEM) studies revealed that 3D printed mortars exhibit pore anisotropy in accordance with the printing direction. However, incorporation of NS in the mixture resulted in improved buildability, thus decreasing pore anisotropy.

ACKNOWLEDGEMENTS

This project received funding from the European Union's Horizon 2020 research and innovation program, as part of Marie Skłodowska-Curie Grant agreement no. 841592.

Project website: www.ultralightcon3d.com

